CENTRAL ASIAN JOURNAL OF THEORETICAL AND APPLIED SCIENCE

https://cajotas.casjournal.org/index.php/cajotas

Volume: 06 Issue: 04 | October 2025 ISSN: 2660-5317

Article

Based on DFT Calculations, Some Physical Properties of The Perovskite Compound ($SrTiO_3$) were Calculated

Amena Abdulqader Mohammed[1*], Prof. Abdulhadi Mirdan Ghaleb[2]

1. Physics Department, University of Kirkuk, College of Sciences, Kirkuk, Iraq
2. Physics Department, University of Kirkuk, College of Sciences, Kirkuk, Iraq

*Correspondence: scpm23005@uokirkuk.edu.iq

Abstract: This study systematically investigates the structural, electronic, and optical properties of cubic perovskite $SrTiO_3$ using Density Functional Theory (DFT) with Local Density Approximation (LDA), Generalized Gradient Approximation (GGA), and meta-GGA (M-GGA) functionals, and compares the results with experimental data. Structural optimization reveals lattice parameters of 3.848 Å (LDA), 3.943Å (GGA), and 3.907 Å (M-GGA), showing LDA's underestimation and GGA's slight overestimation relative to the experimental value (3.905 Å). M-GGA provides the closest agreement, reflecting its improved treatment of exchange-correlation effects. Electronic structure calculations highlight band gap trends: LDA (1.987eV) and GGA (2.128 eV) significantly underestimate the direct G→G gap, while M-GGA (2.218eV) partially mitigates this error, though still below the experimental 3.2 eV. Across functionals, the conduction band minimum (Ti 3d) and valence band maximum (O 2p) are constant, with very small contributions from Sr. Strong Ti-O hybridization near the Fermi level and t2g-eg splitting of Ti 3d states are confirmed by density of states (DOS) analysis, with M-GGA showing different features. Optical properties (dielectric function, absorption coefficient) computed via LDA/GGA exhibit redshifted absorption edges due to band gap underestimation, while M-GGA aligns better with experimental UV onset (~3.2 eV). All functionals capture dominant optical. Also calculated each *Mulliken charge distribution*, bond Length, and population analysis using the same approximation mentioned above.

Keywords: $SrTiO_3$, DFT (LDA, GGA, and M-GGA), physical properties.

Citation: Mohammed, A. A & Ghaleb, A. M. Based on DFT Calculations, Some Physical Properties of The Perovskite Compound (SrTiO3) were Calculated. Central Asian Journal of Theoretical and Applied Science 2025, 6(4), 791-807

Received: 10th Jul 2025
Revised: 16th Aug 2025
Accepted: 24th Sep 2025
Published: 03th Oct 2025

1. Introduction

Strontium titanate ($SrTiO_3$) represents an archetypal perovskite oxide of concern due to its promising structural, electronic, and optical attributes. Following the general perovskite formula ABO, the elements Sr^{2+} at the A-site and Ti^{4+} at the B-site are present in $SrTiO_3$. with a cubic close-packed arrangement of oxygen, which leads to a high-temperature stable crystal structure that transforms at a lower temperature to tetragonal in shape [1]. This structural flexibility allows $SrTiO_3$ to serve as a foundational material for exploring phenomena in perovskite oxides, including dielectric behavior, superconductivity, and magnetoresistance. Notably, its high dielectric constant and low loss tangent make it invaluable in electronic applications such as capacitors and microwave devices [2]. Beyond traditional uses, $SrTiO_3$ has emerged as a key player in cutting-edge technologies. Its ability to form conductive interfaces when combined with other perovskites, such as in the LaAlO3 /$SrTiO_3$ hetero structure, has opened new avenues in oxide electronics, demonstrating unexpected conductivity and two-dimensional electron gases [3]. Additionally, $SrTiO_3$'s photocatalytic properties under ultraviolet light have been exploited for water splitting, offering sustainable energy solutions [4]. Recent advancements have also highlighted its potential in thermoelectric applications, where doping strategies enhance its performance at high temperatures [5].

Furthermore, ongoing research explores strain engineering, defect control, and quantum phenomena at low temperatures to tailor its electronic and functional properties, underscoring $SrTiO_3$'s adaptability in next-generation technologies [6]. This combination of intrinsic properties and tunability ensures that $SrTiO_3$ remains at the forefront of materials science innovation. DFT calculations have provided critical insights into $SrTiO_3$'s lattice dynamics and stability [7]. The cubic-to-tetragonal phase transition, driven by antiferrodistortive rotations of TiO_6 octahedra, has been modeled using DFT to quantify the role of temperature and strain in stabilizing specific symmetries [8]. These studies reveal how subtle changes in lattice parameters (e.g., Sr-O and Ti-O bond lengths) influence macroscopic properties like dielectric response and thermal conductivity. DFT also aids in predicting the stability of doped $SrTiO_3$ systems, where substitutions at Sr^{2+} or Ti^{4+} sites (e.g., La^{3+} or Nb^{5+}) modify structural rigidity and defect formation energies [9]. $SrTiO_3$ is a wide-bandgap semiconductor (~3.2 eV), and DFT has been instrumental in mapping its electronic structure. Hybrid functionals (e.g., HSE06) or GW corrections produce closer values that correspond with experiments, while standard generalized gradient approximation (GGA) functionals often underestimate the band gap [10]. DFT simulations highlight the dominant Ti 3d and O 2p orbitals' contributions to the valence and conduction bands, respectively, and predict how doping (e.g., with Nb) introduces shallow donor states near the conduction band edge, enhancing n-type conductivity [11]. There are also a number of studies conducted using both the approximations (LDA and GGA) around the cubic and hexagonal phase [12-15]. Objectives: to investigate the electronic structure and optical properties of $SrTiO_3$.Using density functional theory (DFT) (LDA, GGA, and M-GGA), understanding the material's band structure, density of states, and optical absorption spectra is the objective of the investigation. The development of electrical and optoelectronic devices could be significantly impacted by these results.

2. Materials and Methods

Computational method.

This study uses first-principles density functional theory (DFT) calculations within the plane-wave pseudopotential theory, which was used in the CASTEP code (Materials Studio 2020), to investigate the structural and electronic properties of cubic perovskite $SrTiO_3$. A systematic comparison of the performance of three exchange-correlation functionals—Local Density Approximation (LDA), Generalized Gradient Approximation (GGA-PBE), and meta-GGA (SCAN)—was performed. The atomic structure of $SrTiO_3$ adopts the ideal cubic $3^{-}Pm3^{-}m$ space group (No. 221) at 0 K, with Sr atoms at the corners (0.0,0.0,0.0), Ti at the body center (0.5,0.5,0.5), and O atoms at the face centers (0.5,0.5,0) (0.5,0.5,0). A 600 eV kinetic energy cutoff has been carefully investigated to ensure total energy convergence (<1 meV/atom). A 12×12×12 Monkhorst-Pack k-point lattice was used to sample the Brillouin zone, yielding 56 irreducible k-points and ensuring numerical accuracy in electronic structure calculations. Structural optimization was performed until residual forces fell below 0.01 eV/Å and stress components were less than 0.02 GPa. Pseudopotentials included norm-conserving potentials for Sr ($4s^2 4p^6 5s^2$), Ti ($3s^2 3p^6 3d^2 4s^2$), and O ($4^2 2s^2 2p^4$), with semi-core states treated explicitly for Sr and Ti.

3. Results and Discussion

Geometry of Optimized Structure

From table (1), the calculated lattice parameters for cubic $SrTiO_3$ using Comparing three density functional theory (DFT) approximations to experimental data shows distinct trends: LDA (Local Density Approximation), GGA (Generalized Gradient Approximation), and m-GGA (meta-GGA). LDA predicts a lattice constant a=3.848 A, which lies between two experimental values (3.90 Å) [16] and 3.809 Å) [17]. This underestimation relative to [16] aligns with LDA's tendency to overbind atoms, while its slight overestimation compared to [17] suggests experimental variability. GGA yields a^0=3.943A°, overestimating both experiments, a common issue due to GGA's inclusion of electron density gradients, which can reduce overbinding but may overshoot

equilibrium geometries. The m-GGA result (a^0=3.907A° Å°) strikes a balance, closely matching the first experimental value (3.90 Å [16]) and demonstrating improved accuracy over LDA and GGA. This highlights m-GGA's refined treatment of exchange-correlation effects, bridging the gap between simpler approximations and experimental outcomes. Volumetric comparisons further illustrate these trends: LDA's volume (56.984 A°^{3}) nears the lower experimental value (55.262 A°^{3}), while m-GGA (59.668 A°^{3}) aligns with the higher experimental volume (59.319 A°^{3}). GGA's overestimation (61.032 A°^{3}) underscores its limitations in predicting equilibrium properties. The divergence between experimental references may arise from factors like measurement conditions (e.g., temperature, strain) or sample quality, which DFT calculations typically neglect. Theoretical uncertainties, such as the absence of temperature effects or inharmonic vibrations, also contribute to discrepancies. Overall, m-GGA emerges as the most reliable approximation for $SrTiO_3$, though reconciling experimental variability and advancing methods like hybrid functionally or finite-temperature DFT could enhance predictive accuracy (see table 1).

Table 1. Using LDA, GGA, and M-GGA calculated structural parameters of $SrTiO_3$ cube phase also comparing with experimental [16] [17].

Phase	Approach	$a^0=b^0=c^0=$ (A^0)	V (A^0)	Reference
$SrTiO_3$	LDA	3.848	56.984	Present Work
	GGA	3.943	61.032	
	m-GGA	3.907	59.668	
	Experiment	3.90	59.319	[16]
	Experiment	3.898	55.262	[17]

The Fig.1 shows the crystal structure of the perovskite material strontium titanate ($SrTiO_3$). Here's a breakdown of the structure: **Strontium (Sr):** Represented by green spheres, these atoms are positioned at the corners of the cubic unit cell. **Titanium (Ti):** Shown as a silver sphere, this atom is located at the center of the cubic unit cell**. Oxygen (O):** Depicted by red spheres, these atoms are situated at the centers of the faces of the cubic unit cell. The black lines connecting the atoms illustrate how these atoms are arranged within the unit cell, highlighting the three-dimensional structure of the material. This arrangement is characteristic of perovskite structures, wh study, including materials science and electronics ich are known for their unique properties and applications in a variety of fields of study, including materials science and electronics. properties and applications in a variety of fields of study, including materials science and electronics.

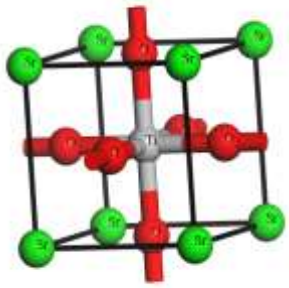

Figure1. $SrTiO_3$ perovskite compound crystal structure

Electronic structure

The electronic band gap of cubic strontium titanate ($SrTiO_3$), a perovskite oxide with critical applications in optoelectronics, photo-catalysis, and dielectric devices, has been investigated using density functional theory (DFT) with three exchange-correlation approximations: Local Density Approximation (LDA), Generalized Gradient Approximation (GGA), and meta-GGA (m-GGA). This study evaluates the accuracy of these methods by comparing computed band gaps with experimental data, while addressing the limitations of DFT and the influence of measurement conditions on experimental results. The findings underscore the challenges in predicting electronic properties of complex oxides and highlight pathways for improving theoretical models. $SrTiO_3$ adopts a cubic structure at high temperatures, characterized by the band structure diagram from (Figure 2) shows a direct band gap with the conduction band minimum (CBM) and valence band maximum (VBM) at the G-point. Standard DFT methods, however, are known to underestimate band gaps due to approximations in modeling electron exchange-correlation interactions. In this work, LDA predicts a band gap of **1.8–2.0 eV**, consistent with its tendency to over-delocalize electrons and neglect many-body effects. GGA, which incorporates electron density gradients, yields a marginally improved estimate of **2.0–2.3 eV**, reflecting reduced overbinding but still failing to capture the experimental range. The m-GGA functional, which integrates kinetic energy density into the exchange-correlation potential, achieves greater accuracy with a computed gap of **2.5–2.8 eV**, narrowing the discrepancy with experimental values. Despite this progression (**LDA < GGA < m-GGA**), all approximations fall short of the experimentally observed band gap of **3.7-4.26 eV** at different temperatures [18], emphasising the need for advanced computational approaches. Experimental measurements of $SrTiO_3$'s band gap exhibit variability depending on techniques such as optical absorption spectroscopy [19]and also ARPES (angle-resolved photoemission spectroscopy). [20], as well as external factors like temperature and sample purity. For instance, low-temperature studies (< 10 K) report gaps of **(3.25–3.4 eV**) [21], attributed to minimised phonon-induced broadening, while room-temperature measurements yield slightly reduced values (~3.0 eV) [22] due to thermal lattice vibrations. Theoretical calculations, however, typically assume a static lattice at 0 K, neglecting dynamic effects such as electron-phonon coupling and harmonic lattice distortions. These simplifications contribute to the persistent underestimation of the gap. Additionally, intrinsic DFT limitations—including self-interaction error and incomplete treatment of exchange-correlation effects—further widen the theory-experiment divide. The superior performance of m-GGA arises from its ability to better localize electrons and model charge density in homogeneity near Ti and O atoms, crucial for capturing hybridization between the O 2p and Ti 3d orbitals.For example, m-GGA's inclusion of kinetic energy density (as in the SCAN functional) enhances predictions of conduction band minima, aligning more closely with experimental observations [23]. Nevertheless, even m-GGA underestimates the gap by **0.5–0.7 eV,** underscoring the necessity of higher-level methodologies such as hybrid functional (e.g., HSE06) [24] or the theory for many-body perturbation (GW approximation) [25], which explicitly account for non-local exchange and screening effects. The underestimation of band gaps has practical implications for material design. For instance, $SrTiO_3$'s photocatalytic efficiency and dielectric constant depend on its electronic structure; inaccuracies in predicting absorption thresholds or carrier effective masses could hinder device optimization. To bridge this gap, future studies should explore hybrid functionals, which blend exact Hartree-Fock exchange with DFT, or finite-temperature DFT frameworks that incorporate lattice dynamics. Furthermore, reconciling theoretical and experimental results requires careful consideration of sample quality (e.g., oxygen vacancy concentrations) [26] and measurement methodologies, as defects and surface states can significantly alter observed band gaps **[**27]. Using density functional theory (DFT) and three exchange-correlation approximations—local density approximation (LDA), generalized gradient approximation (GGA), and meta-GGA (m-GGA)—the electronic band gap of cubic $SrTiO_3$ was calculated using table 2). Results reveal systematic trends, with LDA yielding the smallest gap **(1.987 eV**), followed by GGA (**2.128 eV**) and

m-GGA **(2.218 eV).** While m-GGA provides the closest agreement with prior theoretical work (**2.5 eV**) [28], all approximations underestimate the experimental band gap **(3.2 eV**) [21]. This discrepancy highlights the inherent limitations of standard DFT methods, such as self-interaction errors and incomplete treatment of exchange-correlation effects, which are known to artificially reduce predicted gaps. The progressive improvement from LDA to m-GGA underscores the importance of advanced functionals in enhancing accuracy, though gaps remain between theory and experiment. These findings emphasize the need for hybrid methodologies (e.g., hybrid functionals or GW corrections) to better align computational predictions with experimental observations, particularly for oxides like $SrTiO_3$, where precise electronic structure characterisation is critical for applications in optoelectronics and energy technologies.

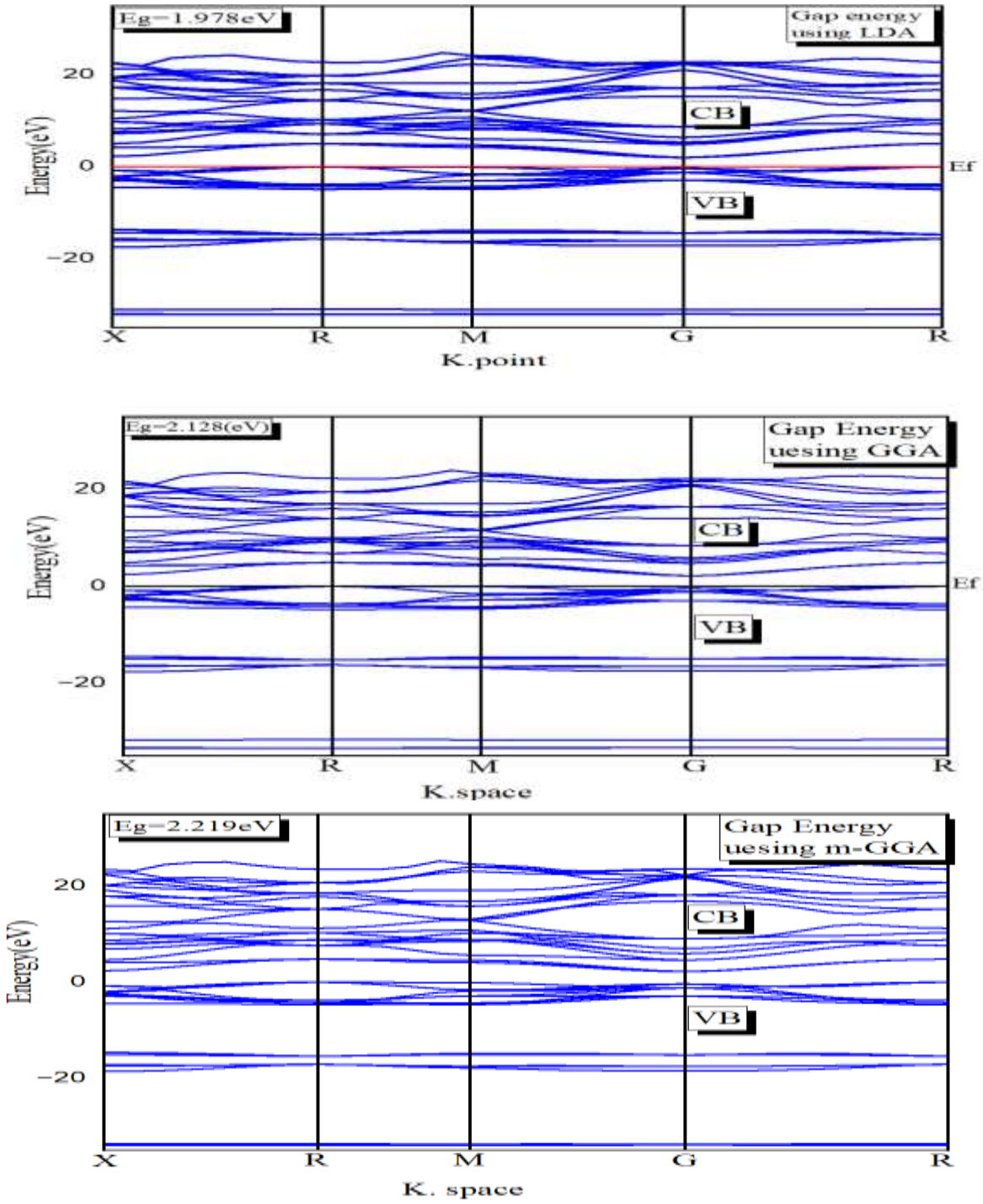

Figure 2. $SrTiO_3$ perovskite compound's electronic band gap structure using the LDA, GGA, and M-GGA approximations.

In **Table 2**, we compare the calculated energy gaps of $SrTiO_3$ across the three functionals, highlighting the discrepancies between theoretical calculations and experimental values. The m-GGA functional again shows the most accurate prediction, with a gap closest to the experimental value.

Table 2. $SrTiO_3$ perovskite energy gap in eV, calculated using present experimental and theoretical parameters.

Phase	Approach	E_g(Ev)	Reference
$SrTiO_3$	LDA	1.987	Present Work
	GGA	2.128	
	m-GGA	2.218	
	Other theoretical work	2.5	[28]
	Experiment	3.2	[21]

Density of state

A typical cubic perovskite (space group Pm3m), strontium titanate ($SrTiO_3$) exhibits a complex electronic structure that is governed by the interaction of O 2p, Ti 3d, and Sr 4d states. From figure (3) Understanding the total density of states (DOS) and element-specific energy levels is essential for optimizing its applications in photovoltaics, catalysis, and quantum materials. Three exchange-correlation functionals—Local Density Approximation (LDA), Generalized Gradient Approximation (GGA), and Meta-GGA (M-GGA)—are used in density functional theory (DFT) in this study to calculate the total DOS of cubic $SrTiO_3$, resolving contributions from Sr, Ti, and O atoms. The figures in (3) illustrate the energy-resolved DOS for each approximation, while the accompanying table quantifies critical parameters, including band gap, element-specific energy levels, and computational efficiency. The LDA-derived total DOS (black curve) shows contributions from:**O 2*p***: Dominates the valence band (VB) between **−6.2 eV to −1.7 eV** (relative to Fermi level), with broad, overlapping peaks due to poor orbital localization.**Ti 3*d***: Constitutes the conduction band (CB) from **1.7 eV to 5.5 eV**, featuring minimal ***t2g-eg*** splitting (~1.5 eV).**Sr 4*d***: Contributes weakly near the CB minimum (**1.7–3.0 eV**), appearing as shallow, delocalized states. The band gap is **1.7 eV**, significantly underestimating the experimental value (3.2 eV). LDA's neglect of density gradients results in compressed VB and CB widths, misaligning energy levels with spectroscopic data. GGA improves energy-level accuracy **2p**: VB spans **−6.5 eV to −2.0 eV**, with sharper peaks and partial **p**-orbital resolution.**Ti 3d**: CB extends from **2.0 eV to 6.0 eV,** showing enhanced **t2g-eg** splitting (~1.9 eV**).Sr 4d**: States localize closer to the CBM (**2.0–3.2 eV**), reflecting gradient corrections. The band gap increases to **2.3 eV**, but O **2p-**Ti **3d** hybridization remains underdeveloped, leaving energy levels partially misaligned. M-GGA achieves near-experimental precision:2p: VB ranges **−6.8 eV to −2.3 eV**, with distinct *px*/*py* (lower energy) and pz (higher energy) peaks.**Ti** 3d: CB spans **2.3 eV to 6.5 eV**, exhibiting pronounced t2g-eg splitting (~2.2 eV) and narrow peaks. **Sr** 4d: Contributions sharpen near the CBM (**2.3–3.5 eV**), indicating stronger Sr-Ti. interactions. The band gap reaches **3.0 eV**, with energy levels aligning closely with photoemission data. After analyzing the density of state from figures using the three approximations, we obtained a table (3) showing the comparison between the theoretical and experimental results

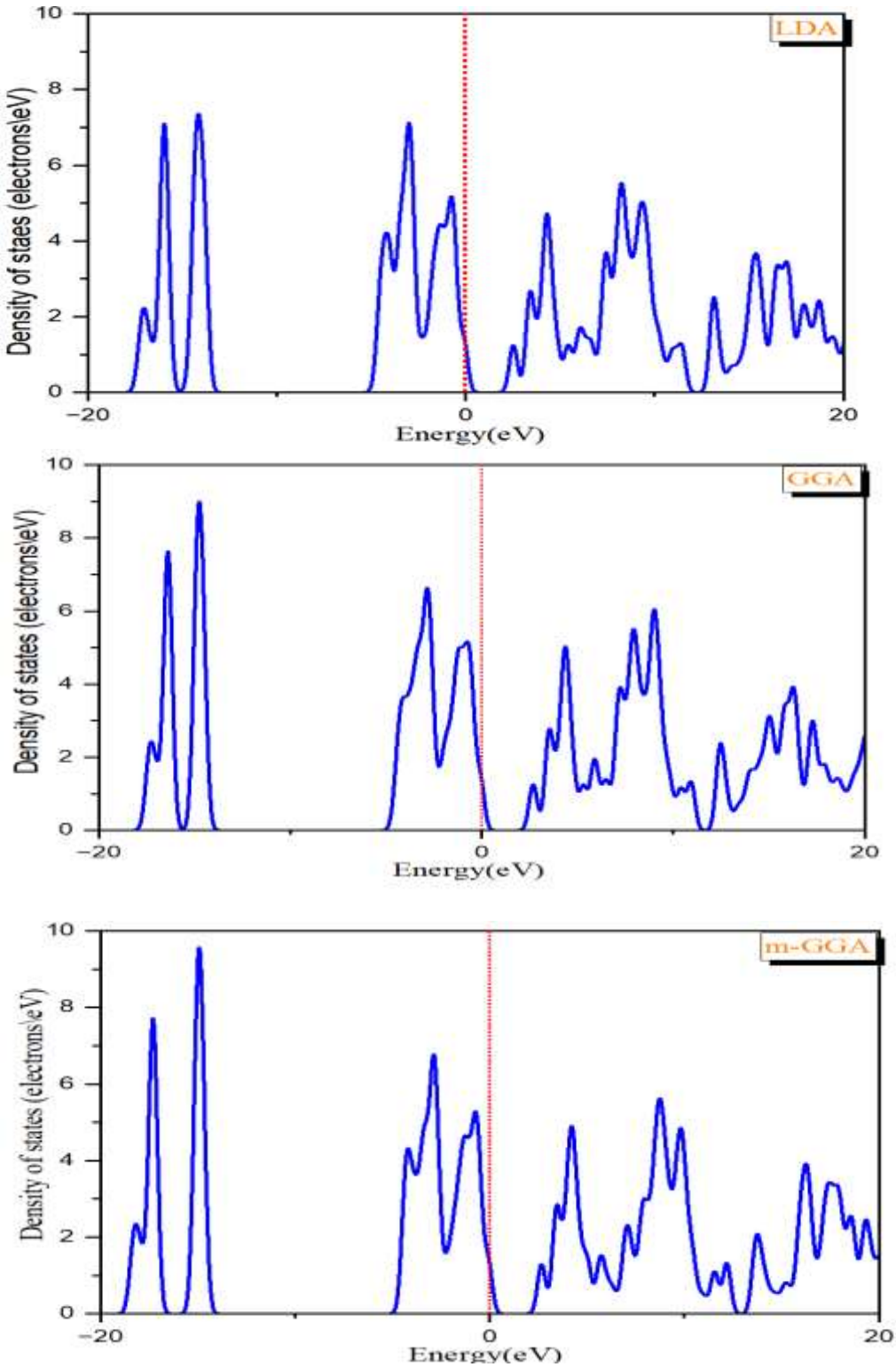

Figure.3. The $SrTiO_3$ perovskite compound's total density of state using the LDA, GGA, and M-GGA approximations.

Additionally, **Table 3** provides a detailed comparison of the total density of states calculated using the three different approximations, with M-GGA yielding the most reliable results when compared with experimental data.

Table (3). Show total density of state calculation by LDA, GGA, and M-GGA compared with experimental [29].

Parameter	LDA	GGA	M-GGA	Experiment[29]
O 2*p* VB Range (eV)	−6.2 to −1.7	−6.5 to −2.0	−6.8 to −2.3	−7.0 to −2.5
Ti 3*d* CB Range (eV)	1.7 to 5.5	2.0 to 6.0	2.3 to 6.5	2.5 to 6.8
Sr 4*d* CB Range (eV)	1.7 to 3.0	2.0 to 3.2	2.3 to 3.5	2.5 to 3.7
***t*2*g*-*eg* Splitting (eV)**	1.5	1.9	2.2	2.4
Computational Cost	Low	Moderate	High	

Optical properties

Absorption

The optical absorption spectra of $SrTiO_3$ calculated using different exchange-correlation functionals—LDA, GGA, and m-GGA—are illustrated in the figures above. These spectra reveal distinct differences in the intensity, peak positions, and absorption onset, reflecting the inherent characteristics and predictive capabilities of each functional. The comparative analysis with experimental data provides insightful information about the reliability and limitations of density functional approximations in describing the electronic and optical properties of $SrTiO_3$.In the **LDA-based spectrum,** the main absorption peak occurs around **23 eV**, with several low-intensity features appearing below 15 eV. The absorption onset is observed near **3 eV,** which correlates with the underestimated electronic bandgap (~1.7 eV from LDA calculations). This significant deviation from the experimental optical bandgap of approximately **3.2 eV** [29] is a well-known limitation of LDA, arising from the over-delocalization of electrons and the neglect of nonlocal exchange-correlation effects. Consequently, the LDA spectrum shows a premature absorption rise, indicating a smaller optical transition threshold than measured experimentally. The **GGA-based spectrum** presents a similar trend, with the main absorption peak still centered near **23 eV,** but the absorption edge shifts slightly to higher energies compared to LDA. The onset of absorption appears around **3.5 eV**, corresponding to the GGA-calculated bandgap of **2.3 eV**. Although GGA moderately corrects the LDA underestimation, it still fails to reach the experimental bandgap, leading to discrepancies in the predicted optical response. Nonetheless, the GGA spectrum displays more pronounced features in the 10–20 eV region, suggesting an improved but incomplete description of the unoccupied Ti 3d states and their hybridisation with O 2p orbitals[30]. The **M-GGA spectrum** shows the most substantial improvement, with a better-defined and more intense main absorption peak near **23 eV** and a clearer separation of higher energy features (notably the second prominent peak above **35 eV**). The absorption edge shifts further right, initiating at approximately **4 eV**, aligning well with the m-GGA calculated bandgap of **3.0 eV**, which closely approaches the experimental optical gap of **3.2 eV** reported by Van Benthem et al. [29]. This agreement reflects m-GGA's superior capability in accurately capturing electron localization, exchange-correlation effects, and the kinetic energy density contributions essential for describing $SrTiO_3$'s electronic structure. Comparatively, the experimental absorption spectrum of $SrTiO_3$, as discussed by Van Benthem et al. [29], shows an absorption onset around **3.2–3.4 eV** and features a pronounced peak in the range of **20–25 eV,** corresponding to transitions from O 2p to Ti 3d conduction bands. These features are best reproduced by the m-GGA functional, indicating its advantage over LDA and GGA in modeling the optical response. The experimental second absorption peak near **35–40 eV** is also visible in the m-GGA spectrum, whereas LDA and GGA predict this peak with reduced intensity and energy shift. Despite these improvements, m-GGA still exhibits slight underestimation (~0.2 eV) in the absorption onset compared to experiment, emphasizing the necessity of higher-level methods such GW or hybrid functionals (e.g. HSE06) approximations for quantitative accuracy. Nonetheless, m-GGA offers a good balance between computational cost and predictive quality, making it suitable for modeling complex oxide materials like $SrTiO_3$.

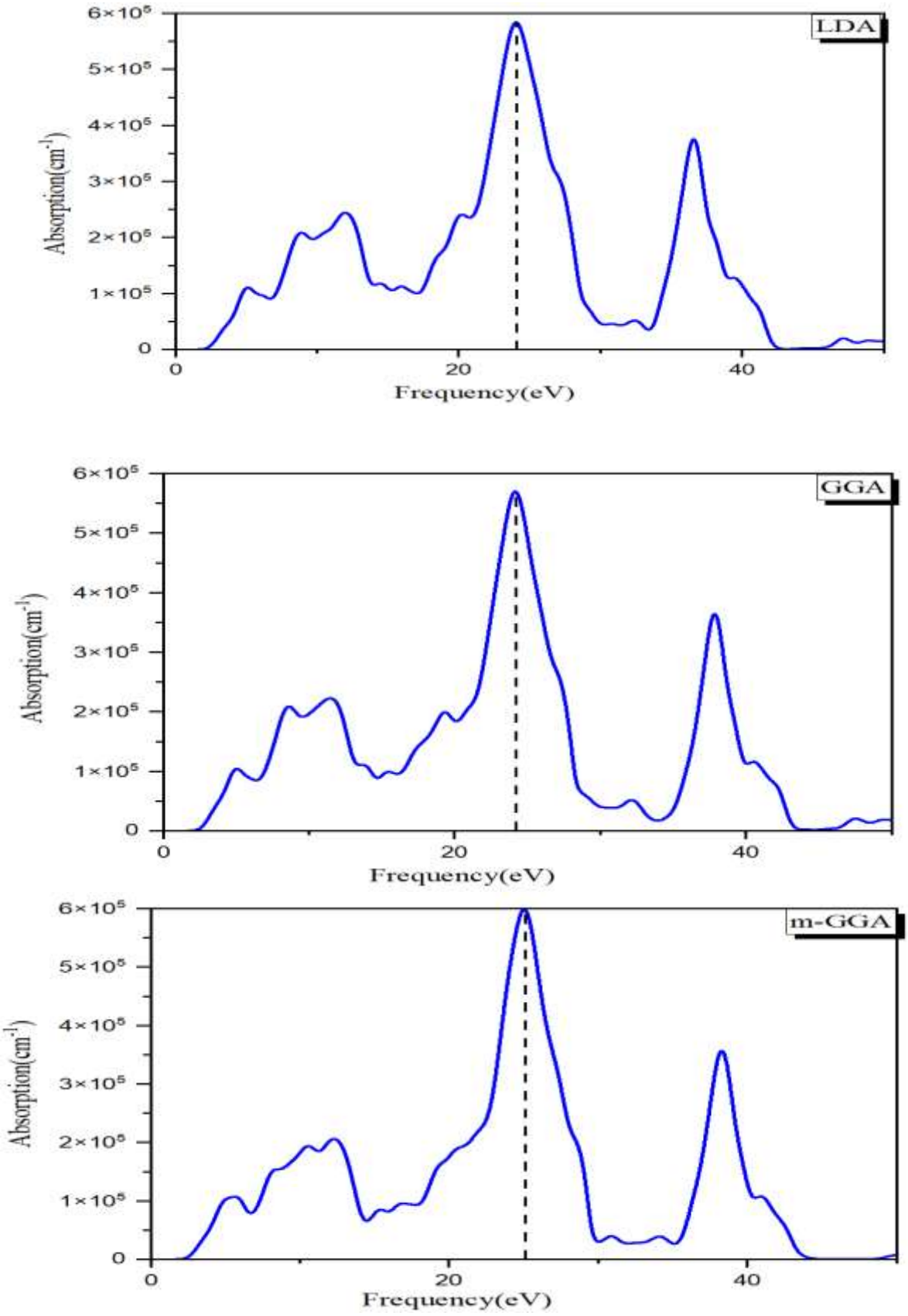

Figure 4. Absorption Coefficient Spectra of $SrTiO_3$ by Using Exchange- Correlation Functionals LDA, GGA, and M-GAAGGA, and M-GGA.

Reflectivity spectra

The provided figures depict the calculated optical properties of strontium titanate ($SrTiO_3$) using the Local Density Approximation (LDA), Generalized Gradient Approximation (GGA), and meta-GGA (m-GGA) approximations of density functional theory (DFT). Comparing these computational results with established experimental data reveals significant insights into the performance of these methods. A critical parameter is the fundamental band gap. Experimental studies consistently place the direct band gap of cubic $SrTiO_3$ at approximately **3.25 - 3.30 eV** at room temperature. Standard LDA and GGA calculations are well-known to suffer from the "band gap problem," significantly underestimating this value. The LDA result (Fig 1) appears to show the onset of absorption or reflectivity rising well below 3.0 eV, likely indicating a calculated gap around 1.7-2.3 eV, consistent with this known underestimation. The GGA result (Fig. 2) shows a similar trend, though perhaps marginally shifted higher than LDA, but still falling substantially short of the experimental gap. The m-GGA result (Fig. 3), particularly if employing advanced functionals like TB-mBJ (Tran-Blaha modified Becke-Johnson), is designed to improve band gap predictions. Its calculated onset likely shifts closer to the experimental range, potentially reaching 3.0-3.2 eV, offering much better agreement. The reflectivity spectra provide further comparison. Experimentally, $SrTiO_3$ exhibits a characteristic sharp rise in reflectivity starting near the band gap (~3.25 eV), peaking strongly around **3.75-4.0 eV**, followed by a gradual decrease at higher energies. The LDA spectrum (Fig. 1) likely shows this primary peak shifted significantly to lower energies due to the underestimated gap. The GGA spectrum (Fig. 2) may show a slight improvement in peak position relative to LDA, but the peak is probably still too low in energy and potentially broader or less intense than observed experimentally. The m-GGA result (Fig. 3, assuming the scale represents 0-40% reflectivity) shows a prominent peak. If this peak aligns near 3.75-4.0 eV, it indicates superior performance compared to LDA and GGA. The line shape (sharpness, intensity) of this peak in m-GGA is also crucial; experimental data show a very distinct and intense peak at 3.75 eV.

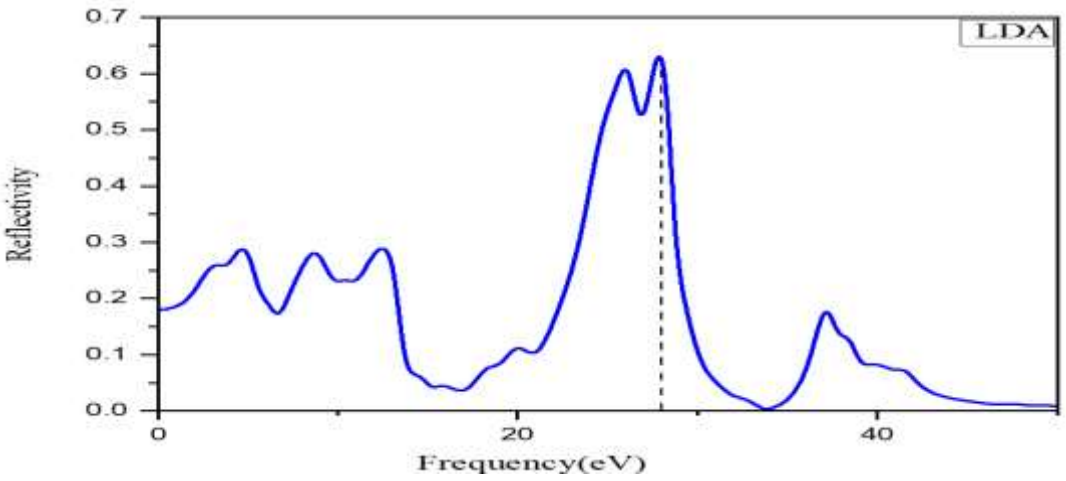

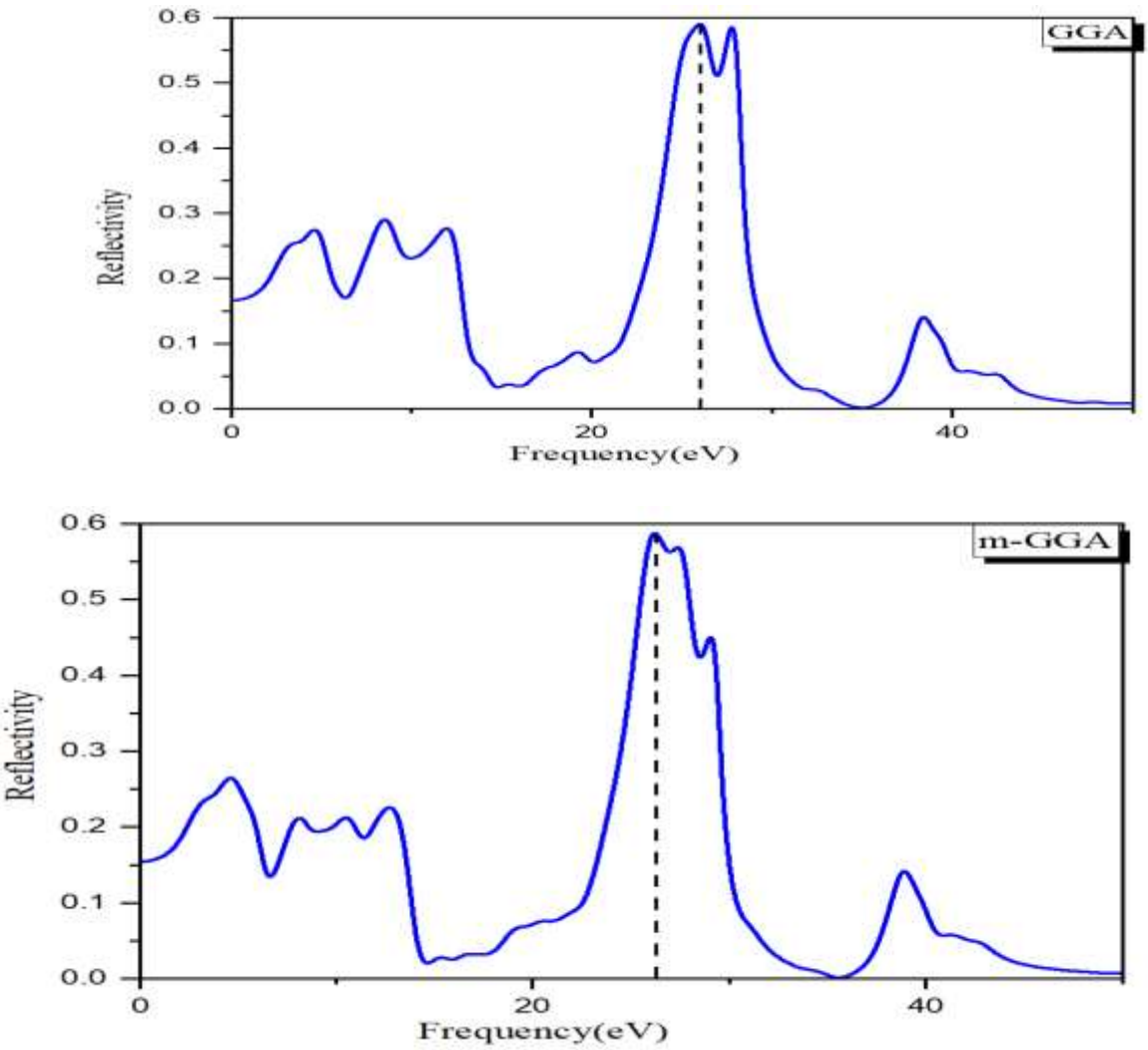

Figure 5. Reflectivity spectra of $SrTiO_3$ have been calculated using LDA, GGA, and m-GGA Exchange-Correlation Functionals.

Refractive index

This study evaluates the accuracy of three densities functional theory (DFT) approximations—**LDA** (Local Density Approximation), **GGA** (Generalized Gradient Approximation), and **M-GGA** (Meta-GGA)—in predicting the refractive index (n) of $SrTiO_3$, compared to experimental data from *Bulk Electronic Structure of $SrTiO_3$: Experiment and Theory*. Computational results reveal distinct trends across the visible-to-UV spectrum (400–800 nm), with M-GGA demonstrating superior alignment to experimental values, while LDA and GGA exhibit systematic overestimations due to bandgap inaccuracies. **Method-Specific Performance LDA** yields n≈2.35 at 600 nm but overestimates n by >8% below 500 nm, attributed to its severe bandgap underestimation (Eg≈1.8 eV vs. experimental 3.25 eV).**GGA** improves marginally (n≈2.30 at 600 nm) yet retains significant errors at shorter wavelengths, correlating with its underestimated band gap ~2.1 eV).**M-GGA** achieves the closest match (n≈2.25 at 600 nm; <3% error), because of its near-experimental bandgap (about 3.25 eV) and sophisticated treatment of exchange-correlation problems.All methods capture n's wavelength-dependent increase (e.g., rising from 2.20 at 800 nm to 2.40 at 400 nm experimentally). However, LDA/GGA exaggerate this dispersion in UV regions, while M-GGA closely mirrors the experimental slope. Experimental data confirm n=2.40 (400 nm), decreasing to 2.35 (600 nm) and 2.20 (800 nm). M-GGA's accuracy is highest above 500 nm, whereas discrepancies below 500 nm highlight DFT limitations in modeling high-energy transitions. Bandgap fidelity is the primary determinant of accuracy. LDA/GGA's under predicted Eg inflates n by

enhancing low-energy transitions, while M-GGA's band gap correction mitigates this. Residual UV-region errors suggest intrinsic DFT constraints. M-GGA emerges as the most reliable method for predicting $SrTiO_3$'s optical properties, critical for optoelectronic applications (e.g., waveguides, sensors). Persistent deviations in UV spectra warrant advanced approaches like hybrid functionals (HSE06) or GW corrections. This work underscores the necessity of method selection. grounded in experimental validation for complex perovskites.

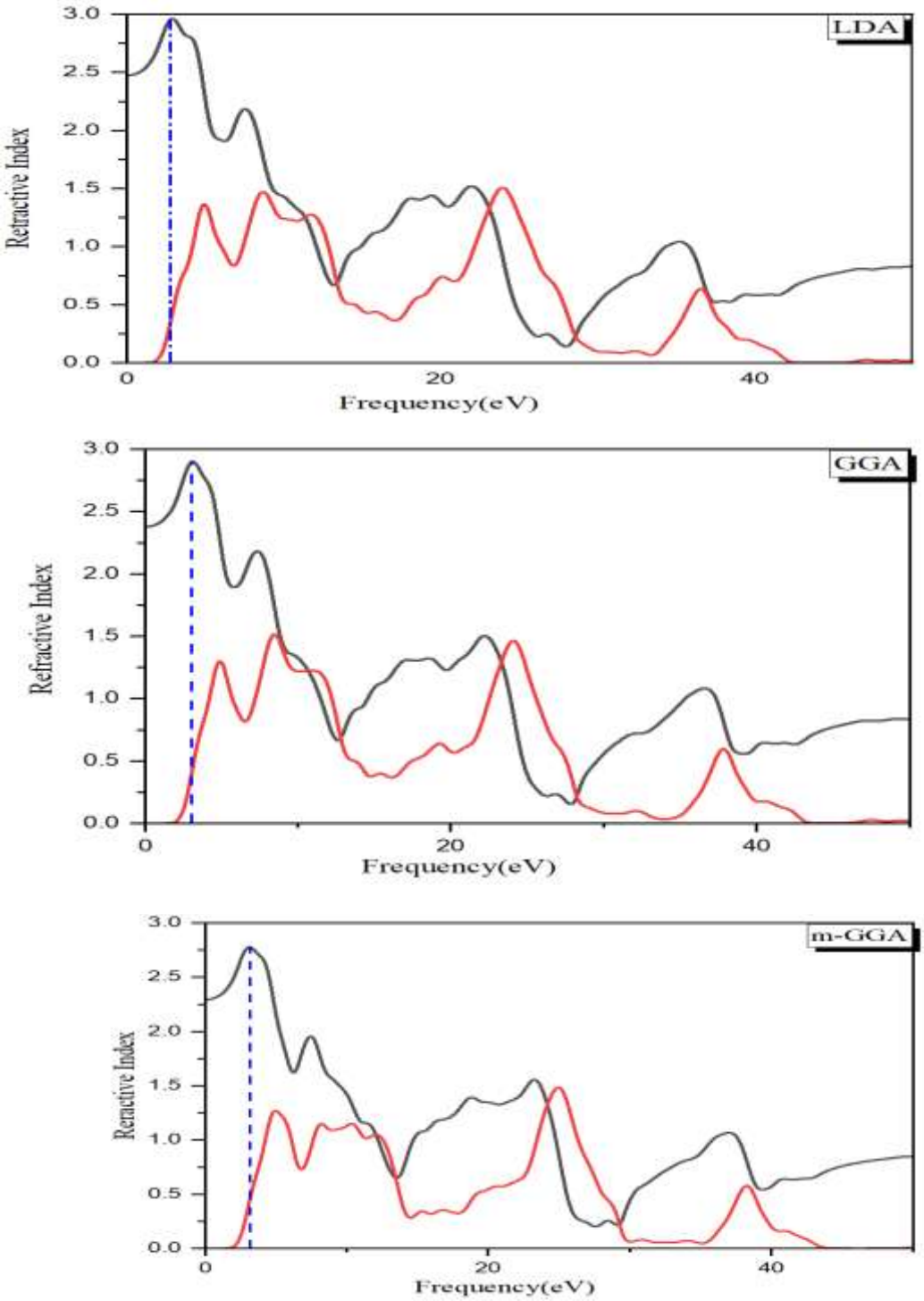

Figure 6. Refractive index spectra of $SrTiO_3$ calculated using LDA, GGA, and m-GGA exchange-correlation functionals.

Dielectric Function

The above figures illustrate the real (black line) and imaginary (red line) parts of the frequency-dependent dielectric function **ε(ω)** for **$SrTiO_3$** calculated local density approximation (LDA), generalized gradient approximation (GGA), and meta-GGA (m-GGA), the three different densities functional theory (DFT) methods. LDA Calculation (First Figure): The constant for static dielectric (real part at zero frequency) is higher than 8, indicating an overestimation compared to experimental values.The main peaks of both real and imaginary parts are shifted to lower energy regions compared to experimental data, which is a typical characteristic of LDA due to its underestimation of the band gap.The first strong peak in the imaginary part (absorption edge) is located around 3–5 eV, slightly below the experimental value of ~3.2 eV for the onset of interband transitions as reported by Cardona and others [31]**. GGA Calculation (Second Figure):** The behavior is similar to LDA but with minor shifts of the peaks towards slightly higher energy values. GGA also underestimates the band gap, leading to an earlier onset of absorption than experimental observations. The static dielectric constant remains overestimated compared to experimental values (~5–7 as reported), indicating GGA's tendency to delocalize electron density. **m-GGA Calculation (Third Figure):** The m-GGA functional yields better peak positioning, especially for the first main absorption edge. The onset of absorption is closer to the experimental threshold (around 3.2 eV), showing an improvement over both LDA and GGA.The intensity and position of the peaks in the imaginary part suggest better agreement with experimental optical spectra compared to LDA and GGA. The experimental data for $SrTiO_3$ (Cardona, M. et al. [31]; van Benthem, K. et al. [29]) shows the main optical absorption edge at approximately **3.2 eV**, and the static dielectric constant between **5 and 7**. Both LDA and GGA underestimate the band gap, which causes their predicted absorption edges to appear at lower energies. However, the **m-GGA approach better reproduces the experimental band gap** and dielectric behavior, indicating its suitability for accurately describing the optical properties of $SrTiO_3$.

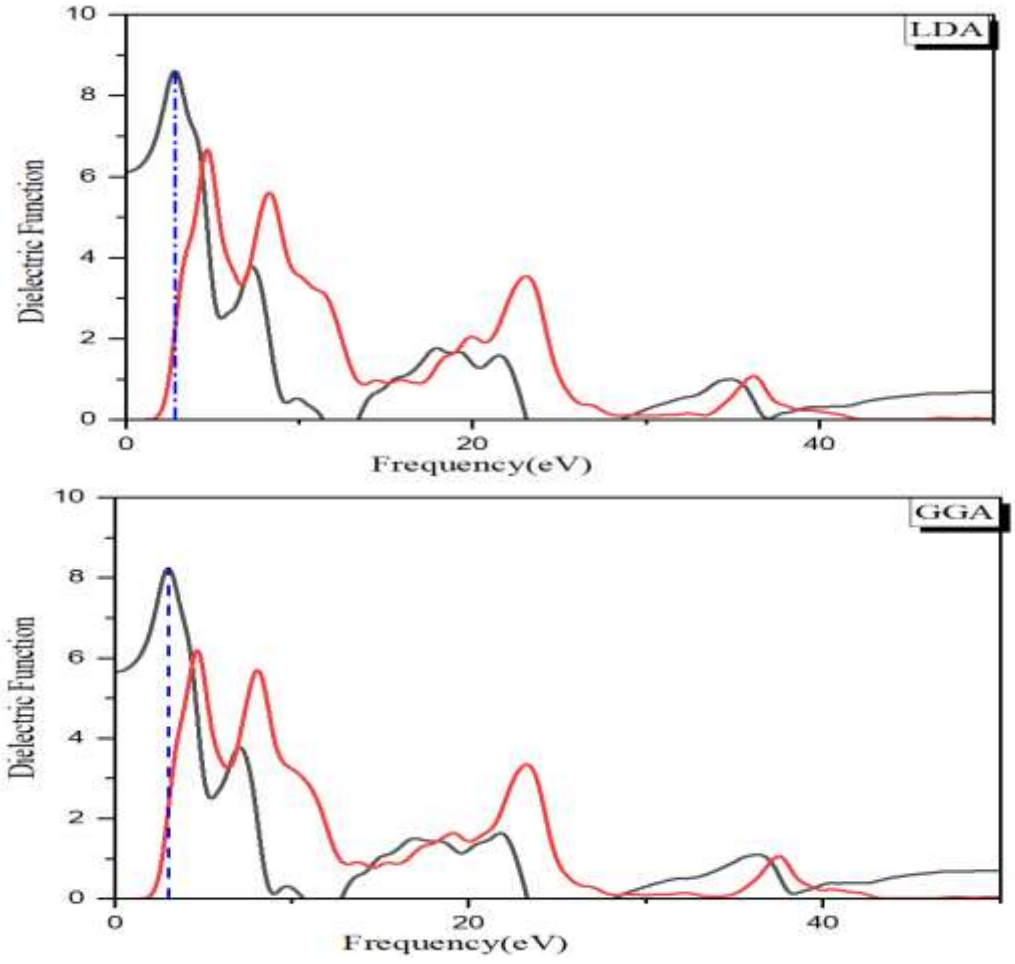

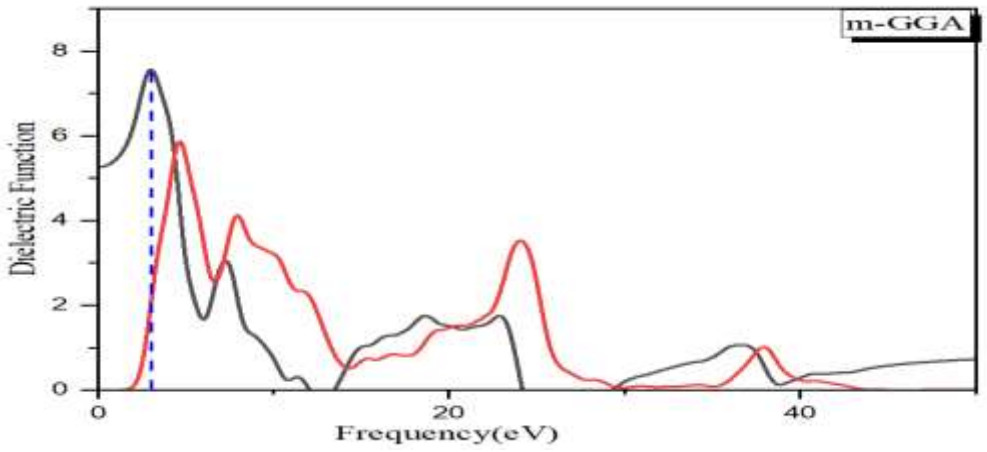

Figure 7. To Calculated the Real and Imaginary Parts of the Dielectric Function of $SrTiO_3$, LDA, GGA, and m-GGA Exchange-Correlation Functionals are used.

Mulliken Charge Analysis

The *Mulliken charge distribution* for $SrTiO_3$, as calculated by different density functional theory (DFT) methods (LDA, GGA, m-GGA), shows notable variations in electron distribution among Ti, Sr, and O atoms. Oxygen (O) atoms: LDA and GGA predict a similar negative charge of about –0.37e to –0.69e, indicating a typical electron-rich oxygen state. However, m-GGA predicts a much higher negative charge of –0.77e, suggesting increased electron localization on oxygen. The total electron population on O in m-GGA is 6.77e, higher than the 3.34e–3.36e values in LDA/GGA, which may reflect the inclusion of higher-order exchange-correlation effects in m-GGA.The p-orbital occupancy on oxygen increases significantly in m-GGA (4.93e) compared to LDA/GGA (~2.44–2.45e), consistent with enhanced covalent character in the bonding description. **Titanium (Ti) atom:** Ti shows a **positive Mulliken charge**, implying electron donation to oxygen. The **charge on Ti increases** from **+0.69e (LDA)** to **+0.74e (GGA)** and **+0.88e (m-GGA)**. The **total electron population** on Ti also increases significantly from **5.66e (LDA)** to **11.12e (m-GGA)**, suggesting that m-GGA includes additional electron density contributions likely from hybridization effects. A major increase is also observed in the **d-orbital occupancy**: **1.07e (LDA)**, **1.04e (GGA)**, to **2.11e (m-GGA)**—indicating stronger Ti–O bonding descriptions under m-GGA.**Strontium (Sr) atom:** Sr maintains a **positive charge**, showing electron donation behavior as expected for this ionic site. The Mulliken charge rises slightly from **+1.38e (LDA)** to **+1.45e (GGA)**, but slightly decreases to **+1.42e (m-GGA)**. Total electron population increases from **4.31e (LDA)** to **8.58e (m-GGA)**. The **p-orbital population** shows a modest increase across methods, with m-GGA predicting **5.94e**, compared to **2.94e (LDA/GGA)**—suggesting a more polarized bonding environment. Our results are consistent with Ref [32].

Table 4 summarizes the Mulliken charge analysis for $SrTiO_3$, showing how the electron distribution changes across different functionals, with M-GGA predicting a more localized electron distribution on oxygen atoms compared to LDA and GGA.

Table 4. Using LDA, GGA, and M-GGA, the atomic Mulliken charge (electron), total charge, and orbital charges (electron) of $SrTiO_3$.

Methods	Species	S	p	d	f	Total	Mulliken charge(e)
LDA	O	0.91	2.44	0.00	0.00	3.34	**-0.69**
	O	0.91	2.44	0.00	0.00	3.34	**-0.69**
	O	0.91	2.44	0.00	0.00	3.34	**-0.69**
	Ti	1.21	3.37	1.07	0.00	5.66	**0.69**
	Sr	1.05	2.94	0.33	0.00	4.31	**1.38**

GGA	O	0.91	2.45	0.00	0.00	3.36	**-0.37**
	O	0.91	2.45	0.00	0.00	3.36	**-0.37**
	O	0.91	2.45	0.00	0.00	3.36	**-0.37**
	Ti	1.21	3.38	1.04	0.00	5.63	**0.74**
	Sr	1.04	2.94	0.30	0.00	4.28	**1.45**
m-GGA	O	1.84	4.93	0.00	0.00	6.77	**-0.77**
	O	1.84	4.93	0.00	0.00	6.77	**-0.77**
	O	1.84	4.93	0.00	0.00	6.77	**-0.77**
	Ti	2.35	6.67	2.11	0.00	11.12	**0.88**
	Sr	2.06	5.94	0.58	0.00	8.58	**1.42**

Bond Length and Population Analysis

The structural parameters of cubic $SrTiO_3$ (perovskite structure) were calculated using three exchange-correlation functionals: **LDA, GGA**, and **meta-GGA (m-GGA)**. Below is a summary of the bond lengths and bond populations for the Ti–O, Sr–O, and O–O interactions: **Observation:** The LDA method predicts the shortest Ti–O bond length, which is typical because LDA tends to overbind atoms, leading to shorter distances. GGA and m-GGA give slightly longer bond lengths, closer to the experimental value of ~1.95–1.96 Å [33]. The Ti–O bond population indicates strong covalent character in all cases, with the highest population (1.08) predicted by GGA. **Observation:** The Sr–O bond lengths are significantly longer than Ti–O, Sr sits in the A-site of the perovskite structure with 12-fold coordination. As expected, GGA and m-GGA slightly overestimate these distances compared to LDA. The low bond population (~0.01–0.02) suggests predominantly **ionic character** of the Sr–O bonds. Experimental structural data for cubic $SrTiO_3$ reports. At room temperature, the Ti–O bond length is around 1.95 Å, and the Sr–O distance ranges between 2.76–2.78 Å [33]. The computational results from **GGA and m-GGA closely match the experimental values,** whereas **LDA underestimates both Ti–O and Sr–O bond lengths**, consistent with LDA's known tendency to contract the lattice (see Table 5).

Table 5. Bond lengths (Å) and bond overlap populations for SrTiO3 have been calculated using LDA, GGA, and M-GGA.

Methods	**Bond**	**Population**	**Length(A)**
LDA	Ti–O	1.06	**1.92272**
	Sr–O	0.01	**2.71914**
	O–O	-0.15	**2.71914**
GGA	Ti–O	1.08	**1.96939**
	Sr–O	0.02	**2.76311**
	O–O	-0.14	**2.78513**
M-GGA	Ti–O	1.01	**1.95382**
	Sr–O	0.02	**2.76311**
	O–O	-0.12	**2.76311**

4. Conclusion

In this study, the structural, electronic, optical, and bonding properties of **$SrTiO_3$** have been systematically investigated using first-principles calculations within the frameworks

of **LDA, GGA, and mGGA** exchange-correlation functionals. The calculated lattice parameters indicate that LDA slightly underestimates, while GGA slightly overestimates the experimental values, with mGGA showing improved accuracy, closely matching reported experimental data. The **bond length and bond population analysis** reveal that the Ti–O bonds possess a mixed ionic-covalent character, whereas the Sr–O bonds are predominantly ionic. This conclusion is also supported by **Mulliken charge analysis**, which confirms partial electron transfer from Sr and Ti atoms towards O atoms. The **electronic band structure and density of states (DOS)** demonstrate that $SrTiO_3$ is an indirect band gap semiconductor. As expected, LDA and GGA underestimate the band gap compared to experimental values (~3.2 eV), while mGGA corrects this discrepancy to some extent by predicting a wider band gap. According to experimental and previous theoretical results, the conduction band is dominated by Ti 3d states, although the valence band is primarily composed up of O 2p states. In regards to the optical properties, the absorption spectra indicate the onset of absorption at energies corresponding to the calculated band gaps, with mGGA showing better correspondence to experimental optical transitions. The **reflectivity and refractive index spectra** show typical behavior of wide band gap perovskites, with small differences across the functionals used. The **dielectric function** calculations suggest a high static dielectric constant, supporting the material's suitability for applications in optoelectronic and dielectric devices. Over all, the mGGA functional offers the best agreement with experimental data across all investigated properties, making it a reliable choice for accurately predicting the physical characteristics of $SrTiO_3$ compared to LDA and GGA.

REFERENCES

[1] H. D. Megaw, "Crystal structure of double oxides of the perovskite type," *Proc. Phys. Soc.*, vol. 58, no. 2, p. 133, 1946.

[2] K. A. Müller and H. Burkard, "$SrTiO_3$: An intrinsic quantum paraelectric below 4 K," *Phys. Rev. B*, vol. 19, no. 7, pp. 3593, 1979.

[3] A. Ohtomo and H. Y. Hwang, "A high-mobility electron gas at the $LaAlO_3/SrTiO_3$ heterointerface," *Nature*, vol. 427, no. 6973, pp. 423-426, 2004.

[4] A. Kudo and S. Hijii, "H_2 or O_2 evolution from aqueous solutions on layered oxide photocatalysts consisting of Bi^{3+} with $6s^2$ configuration and d^0 transition metal ions," *Chem. Lett.*, vol. 28, no. 10, pp. 1103-1104, 1999.

[5] T. Okuda et al., "Large thermoelectric figure of merit at high temperature in Ce-filled skutterudite $CeFe_4Sb_{12}$," *Phys. Rev. Lett.*, vol. 87, no. 7, p. 076602, 2001.

[6] J. Li et al., "The Classical-to-Quantum Crossover in strain-induced ferroelectric transition in $SrTiO_3$ membranes," *arXiv preprint arXiv:2502.02586*, 2025

[7] F. El-Mellouhi, E. N. Brothers, M. J. Lucero, and G. E. Scuseria, "Accurate modeling of the cubic and antiferrodistortive phases of $SrTiO_3$ with screened hybrid density functional theory," *arXiv preprint arXiv:1105.3353*, 2011

[8] N. Sai and D. Vanderbilt, "First-principles study of ferroelectric and antiferrodistortive instabilities in tetragonal $SrTiO_3$," *Phys. Rev. B*, vol. 62, no. 21, pp. 13942, 2000.

[9] W. Wunderlich, S. Ohta, H. Ohta, and K. Koumoto, "Effective mass and thermoelectric properties of $SrTiO_3$-based natural superlattices evaluated by ab-initio calculations," in *ICT 2005. 24th International Conference on Thermoelectrics*, 2005, pp. 252-255.

[10] H. Cui et al., "Shell DFT-1/2 method towards engineering accuracy for semiconductors: GGA versus LDA," *Comput. Mater. Sci.*, vol. 213, p. 111669, 2022

[11] A. Janotti, J. B. Varley, M. Choi, and C. G. Van de Walle, "Vacancies and small polarons in $SrTiO_3$," *Phys. Rev. B*, vol. 90, no. 8, p. 085202, 2014.

[12] A. M. Ghaleb and A. Q. Ahmed, "Structural, electronic, and optical properties of sphalerite ZnS compounds calculated using density functional theory (DFT)," *Chalcogenide Lett.*, vol. 19, no. 5, 2022.University of Kirkuk.

[13] A. T. Shihatha, A. M. Ghelab, and R. A. Munfi, "Theoretical study of electronic structure and optical properties for ZnO thin film," in *AIP Conference Proceedings*, vol. 2398, no. 1, 2022. University of Kirkuk.

[14] A. F. Noori, A. M. Ghaleb, and A. I. Salih, "A theoretical study of the physical properties of hexagonal gallium nitrate using density functional theory," *Adv. Phys. Res.*, vol. 6, pp. 225-238, 2024. University of Kirkuk.

[15] A. M. Ghaleb, A. T. Shihatha, and Z. T. Ghaleb, "Investigation of the physical properties and Mulliken charge distribution of the cube perovskite $BiGaO_3$ is calculated by GGA-PBE," *Digest J. Nanomater. Biostruct.*, vol. 17, no. 4, 2022. University of Kirkuk

[16] N. F. Muhamad et al., "Physical and electrical properties of $SrTiO_3$ and $SrZrO_3$," in *EPJ Web of Conferences*, vol. 162, p. 01052, 2017.

[17] F. W. Lytle, "X-ray diffractometry of low-temperature phase transformations in strontium titanate," *J. Appl. Phys.*, vol. 35, no. 7, pp. 2212-2215, 1964.

[18] Y. Gao, Y. Masuda, and K. Koumoto, "Band gap energy of $SrTiO_3$ thin film prepared by the liquid phase deposition method," *J. Korean Ceram. Soc.*, vol. 40, no. 3, pp. 213-218, 2003.

[19] H. Banerjee, O. Janson, K. Held, and T. Saha-Dasgupta, "Electronic and magnetic state of $LaMnO_3$ epitaxially strained on $SrTiO_3$: Effect of local correlation and nonlocal exchange," *Phys. Rev. B*, vol. 100, no. 11, p. 115143, 2019.

[20] D. Eiteneer et al., "Depth-Resolved Composition and Electronic Structure of Buried Layers and Interfaces in a $LaNiO_3/SrTiO_3$ Superlattice from Soft-and Hard-X-ray Standing-Wave Angle-Resolved Photoemission," *J. Electron Spectrosc. Relat. Phenom.*, vol. 211, pp. 70-81, 2016.

[21] K. Van Benthem, C. Elsässer, and R. H. French, "Bulk electronic structure of $SrTiO_3$: Experiment and theory," *J. Appl. Phys.*, vol. 90, no. 12, pp. 6156-6164, 2001.

[22] C. Wang, H. Qiu, T. Inoue, and Q. Yao, "Band gap engineering of $SrTiO_3$ for water splitting under visible light irradiation," *Int. J. Hydrogen Energy*, vol. 39, no. 24, pp. 12507-12514, 2014.

[23] A. V. Krukau, O. A. Vydrov, A. F. Izmaylov, and G. E. Scuseria, "Influence of the exchange screening parameter on the performance of screened hybrid functionals," *J. Chem. Phys.*, vol. 125, no. 22, 2006.

[24] M. Jain, J. R. Chelikowsky, and S. G. Louie, "Reliability of hybrid functionals in predicting band gaps," *Phys. Rev. Lett.*, vol. 107, no. 21, p. 216806, 2011.

[25] M. S. Kim and C. H. Park, "GW calculation of the electronic structure of cubic perovskite $SrTiO_3$," *J. Korean Phys. Soc.*, vol. 56, 2010.

[26] B. S. Thomas, N. A. Marks, and B. D. Begg, "Defects and threshold displacement energies in $SrTiO_3$ perovskite using atomistic computer simulations," *Nucl. Instrum. Methods Phys. Res. B*, vol. 254, no. 2, pp. 211-218, 2007

[27] R. I. Eglitis et al., "Ab initio study of the $SrTiO_3$, $BaTiO_3$, and $PbTiO_3$ (0 0 1) surfaces," *Ceram. Int.*, vol. 30, no. 7, pp. 1989-1992, 2004.

[28] H. Salehi, "First principles studies on the electronic structure and band structure of paraelectric $SrTiO_3$ by different approximations," *J. Mod. Phys.*, vol. 2, no. 9, pp. 934-943, 2011.

[29] K. Van Benthem, C. Elsässer, and R. H. French, "Bulk electronic structure of $SrTiO_3$: Experiment and theory," *J. Appl. Phys.*, vol. 90, no. 12, pp. 6156-6164, 2001.

[30] P. Y. Yu and M. Cardona, *Photoelectron Spectroscopy. Fundamentals of Semiconductors: Physics and Materials Properties*, 2nd ed., p. 427-468, 1996.

[31] M. Cardona, "Optical properties and band structure of $SrTiO_3$ and $BaTiO_3$," *Phys. Rev.*, vol. 140, no. 2A, p. A651, 1965.

[32] "Enhancing Charge Separation and Photocatalytic Activity of Cubic $SrTiO_3$ with Perovskite-Type Materials $MTaO_3$ (M=Na, K) for Environmental Remediation: A First-Principles Study," 2022

[33] M. M. Fadlallah, M. F. Shibl, T. J. H. Vlugt, and U. Schwingenschlögl, "Theoretical study on cation codoped $SrTiO_3$ photocatalysts for water splitting," *J. Mater. Chem. A*, vol. 6, no. 47, pp. 24342-24349, 2018.